Multifunctional holographic elements for surface measurements

Erez Hasman
Nir Davidson
A. A. Friesem
Weizmann Institute of Science
Department of Electronics
Rehovot 76100, Israel

Abstract. A novel single multifunctional holographic optical element is incorporated into a surface measurement system. As a result the system is lightweight, compact, and simpler than conventional ones. Numerical calculation reveals that submicron resolutions are possible both in the horizontal and vertical directions. Finally, experimental results demonstrate the feasibility of the approach.

Subject terms: multifunctional holographic elements; surface measurements; autofocus error detection.

Optical Engineering 31(2), 363-368 (February 1992).

1 Introduction

The increasing need for noncontact surface displacement and profile measurements that require high horizontal and vertical resolutions has led to the development of several electro-optical systems. These systems incorporate interferometric methods,[1] speckle techniques,[2] Moire deflectometry,[3] triangulation,[4] and focus error detection.[5,6] This last technique is the basic principle of the confocal scanning optical microscope,[7] which has become widely used as an imaging and measurement tool, especially for semiconductors and biological materials. In general, all the systems are cumbersome, include complex optics, and, as a result, are costly.

We developed a novel system for surface profile measurements, based on autofocus error detection. This system's main element is a single multifunctional holographic optical element (MHOE). As a result, the system has only a few optical components, is lightweight and compact, and can offer submicron resolutions both in the horizontal and vertical direction. Moreover, the manufacture of the system is simpler than the present systems, which could result in a substantial cost reduction.

2 Basic Principle of the Measuring System

The operation of our surface profile measuring system is described with the aid of Fig. 1. A spherical wave diverging from point L impinges on the MHOE, from which a first-order diffracted wave converges to point S where a sample to be tested is located. The sample reflects the focused wave back to the MHOE, from which a second diffracted spherical wave converges to point P where a pinhole is located. A detector, whose aperture is limited by the pinhole, detects all the light passing through this pinhole. When the sample is placed accurately at the focused spot S, the reflected spherical wave reconstructs a nonaberrated spherical wave converging to a small focused spot that will pass through the pinhole. If the sample is not at the exact focused spot S, it reflects an aberrated spherical wave, resulting in a large aberrated spot P, most of which will be blocked by the pinhole; the detected light levels will be lower, indicating a focus error. By moving the sample along the z axis, using micrometers and stepper motors (in the feedback mode), until a maximum signal is obtained at the detector, the local surface profile can be measured.

For the MHOE to function as described above, it is recorded with the arrangement shown schematically in Fig. 2. The recording is done with two separate exposures. In the first exposure, a spherical wave that converges to point S interferes with a diverging spherical wave emerging from point L. In the second exposure, the converging spherical wave interferes with a diverging spherical wave that emerges from point P.

3 Optical Performance Analysis

The system can be evaluated by resorting to a simple geometrical analysis or to physical optics considerations. For the evaluation, we will use Fig. 3, which is confined to the optical part of the system. For simplicity, an on-axis configuration is chosen in which the illuminating laser source

Paper 2979 received Aug. 13, 1990; accepted for publication July 5, 1991.

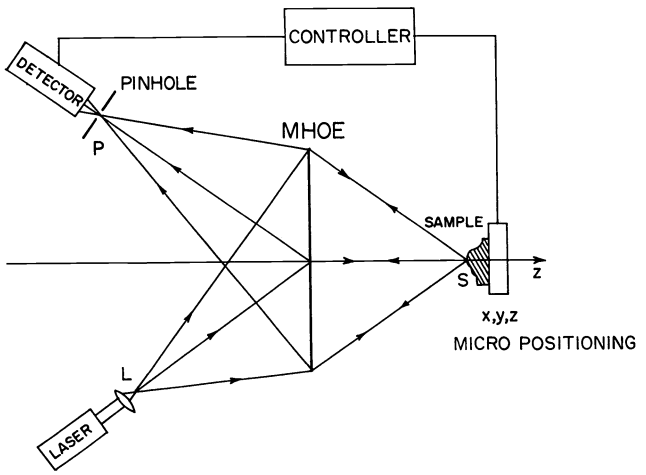

Fig. 1 Basic surface profile measuring system.

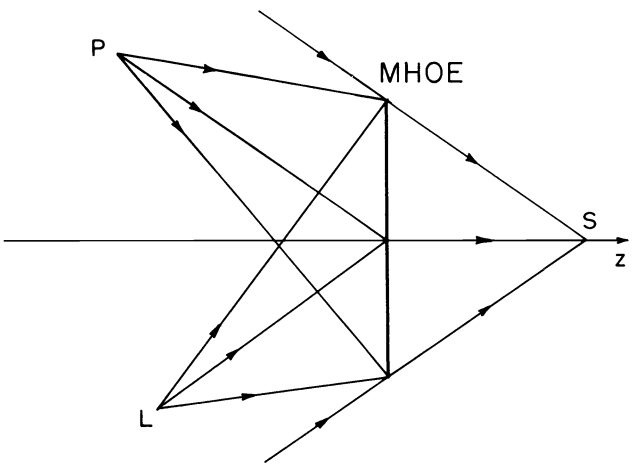

Fig. 2 The recording geometry for the MHOE.

and the detector pinhole are located the same distance from the MHOE. The diameter of the MHOE is D, the diameter of the detector pinhole is D_{ph}, the distance between the MHOE and the source-pinhole plane is R_D, the distance between the MHOE and the focused spot is R_S, and the distance between the MHOE and the sample is R'_S, where $R'_S = R_S + \Delta$, and Δ is the sample displacement from the exact focus. The basic imaging equation for such an optical system, when the sample is at the exact focus, is given by

$$\frac{1}{R_S}+\frac{1}{R_D}=\frac{1}{f} , \tag{1}$$

where f is the focal length of the MHOE. When the sample is displaced from exact focus by Δ, then the imaging relation is

$$\frac{1}{R''_S}+\frac{1}{R'_D}=\frac{1}{f} , \tag{2}$$

where we assumed an ideal reflection (mirror-like) from the sample, so the location for the new effective point source

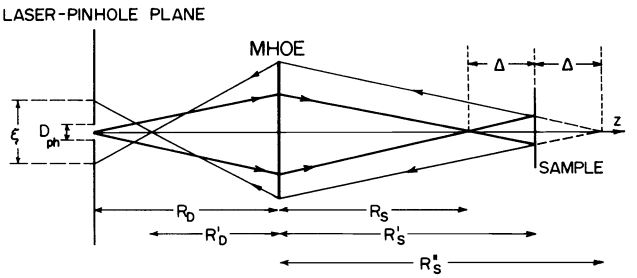

Fig. 3 The geometry and parameters for a simplified optical arrangement.

of the reflected spherical wave becomes $R''_S = R_S + 2\Delta$ and R'_D is the image distance of this point.

From simple geometric considerations, the size of the geometrical spot at the pinhole plane is given by

$$\xi = D\left(\frac{R_D}{R'_D}-1\right) . \tag{3}$$

Inserting R_D and R'_D from Eqs. (1) and (2) into Eq. (3) yields

$$\xi = D\left[\frac{1+2\Delta/(R_S-f)}{1+2\Delta/R_S}-1\right] . \tag{4}$$

Assuming $\Delta << (R_S - f)$ (small displacement) and expanding Eq. (4) by a Taylor series [retaining only the first order in $2\Delta/(R_S-f)$ and $2\Delta/R_S$, yields

$$\xi \simeq \left[\frac{2Df}{R_S(R_S-f)}\right]\Delta . \tag{5}$$

We assume that the minimum displacement $\Delta_{\min}$ that can be detected by such a system, is that for which the geometrical spot ξ is some fraction η of D_{ph}. The actual value of η depends on the accuracy of the detector, the stability of the optical system, and the signal processing used. It will be calculated and discussed later using physical optics considerations, where values smaller than one will be shown to be reasonable. Under this assumption we get

$$\Delta_{\min} \simeq \eta D_{ph} f_{\#S} \cdot \frac{(R_S-f)}{2f} , \tag{6}$$

where $f_{\#S} = R_S/D$.

When the pinhole diameter is close to the diameter of the diffraction-limited spot of the system, $D_{DL} \simeq 2\lambda f_{\#D}$, where $f_{\#D} = R_D/D$ and λ is the wavelength of the illumination laser source; then $\Delta_{\min}$ is given by

$$\Delta_{\min} \simeq \eta \lambda f_{\#D} f_{\#S}\left(\frac{R_S-f}{f}\right) . \tag{7}$$

Using low $f_{\#}$ ($f_{\#D} \simeq f_{\#S} \simeq 1/2$), $\lambda \simeq 0.5$ μm, $R_S = 2f$, and $\eta < 1$, Eq. (7) yields

$$\Delta_{\min} < \frac{1}{8}\mu\text{m} .$$

It is therefore possible to measure the surface displacements with a submicron resolution.

The optical performance of the system can be also evaluated by resorting to physical optics considerations. Again, assuming mirror-like reflections from the sample, the arrangement shown in Fig. 3, and a paraxial approximation, then the field amplitude emerging from the MHOE plane is given by

$$U_T \simeq U_M \cdot U_S = \mathrm{circ}\left(\frac{2r}{D}\right) \cdot \exp\left[-i\frac{\pi}{\lambda}\left(\frac{1}{R_S''} - \frac{1}{f}\right) r^2 \right] , \qquad (8)$$

where $U_M \simeq \exp[i(\pi/\lambda f)r^2]\mathrm{circ}(2r/D)$ is the transmittance of the MHOE and $U_S \simeq \exp[-i(\pi/\lambda R_S'')r^2]$ is the diverging spherical wave emerging from the point distanced R_S'' from the MHOE, with r the radial coordinate in the MHOE plane.

The intensity distribution at the pinhole plane denoted by $I_D(r_D)$ is given by the Fresnel diffraction integral[8,9]:

$$I_D(r_D) \propto \frac{1}{R_D^2} \left| \int_0^{D/2} r U_T(r) \cdot \exp\left(-i\frac{\pi}{\lambda R_D} r^2 \right) \cdot J_0\left(\frac{2\pi r_D}{\lambda R_D} r\right) \mathrm{d}r \right|^2 , \qquad (9)$$

where r_D is the radius coordinate in the pinhole plane and J_0 is the zero-order Bessel function. The relative total power that passes through the pinhole to the detector can be determined by integrating the intensity distribution $I_D(r_D)$ of Eq. (9) over the pinhole diameter D_{ph}. The detected signal, denoted by P_D, is proportional to the total power and is given by

$$P_D \propto \int_0^{D_{ph}/2} I_D(r) r \, \mathrm{d}r \ . \qquad (10)$$

The values of $I_D(r_D)$ and P_D of Eqs. (9) and (10) are found by numerical integration.

As an illustration, we consider an optical system with parameters of $R_D = R_S = 20$ mm, $f = 10$ mm, $D = 10$ mm, and $\lambda = 0.5145$ μm, and use Eqs. (9) and (10) to determine the intensity distribution and the detected signal. The results are given in Figs. 4, 5, and 6. Figure 4 shows the intensity distribution $I_D(r_D)$, at the detector plane, for three sample displacements $\Delta = 0$, 3, and 6 μm. As Δ increases the peak intensity is reduced and the distribution spreads. Figure 5 shows the relative total power as a function of the sample displacement Δ for four pinhole diameters $D_{ph} = 0.2$, 2, 6, and 10 μm. As shown, the measurement accuracy improves as the pinhole diameter is reduced. The improvement is significant as the pinhole diameter approaches the diffraction-limited size of $D_{ph} \simeq 2$ μm. Below the diffraction limit, the improvement is small. Finally, a magnified portion of the graph in Fig. 5 for a pinhole diameter of 2 μm is shown in Fig. 6. From this figure the minimal detectable displacement $\Delta_{\min}$ can be determined once the accuracy of the detected signal is known. For example, if the accuracy is 1%, $\Delta_{\min}$ is about 0.5 μm.

Now, using Eq. (6) and the data from Fig. 6, we calculated the fraction constant η as a function of the accuracy of the detector. The results are shown in Fig. 7, along with

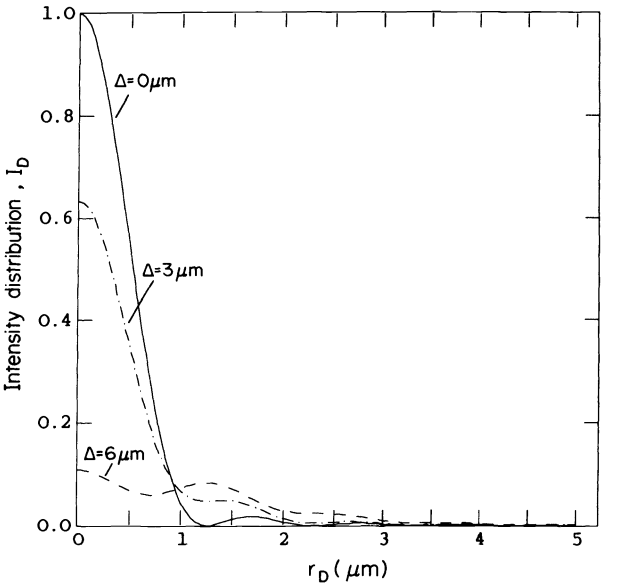

Fig. 4 The intensity distribution at the detector plane for three sample displacements.

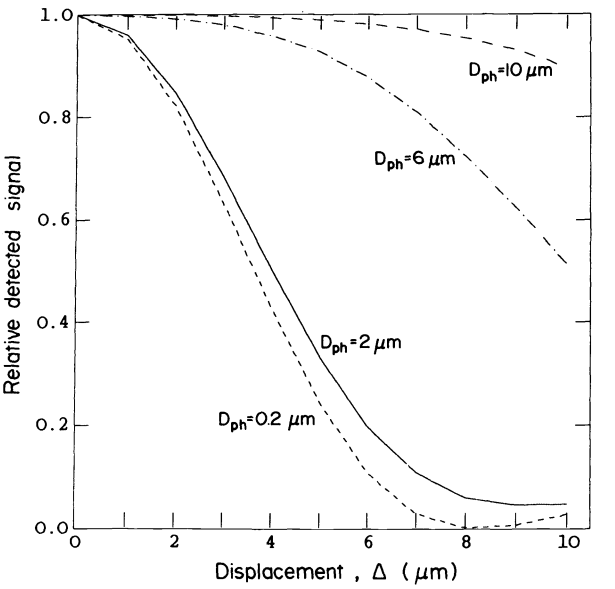

Fig. 5 The detected signal as a function of sample displacement for four pinhole diameters.

the corresponding minimal detectable displacement. As is evident, for a typical detector accuracy of less than 5%, then η is less than one, justifying the assumption we made in the geometrical optic analysis.

4 Realization and Experimental Results

A single MHOE was recorded according to the procedure described earlier and with the arrangement of Fig. 2. An argon laser operating at a wavelength of 0.5145 μm served as the illumination source and a bleached Agfa 8E56 photographic plate was used for recording the element. The exposure energy of both the object and the reference waves

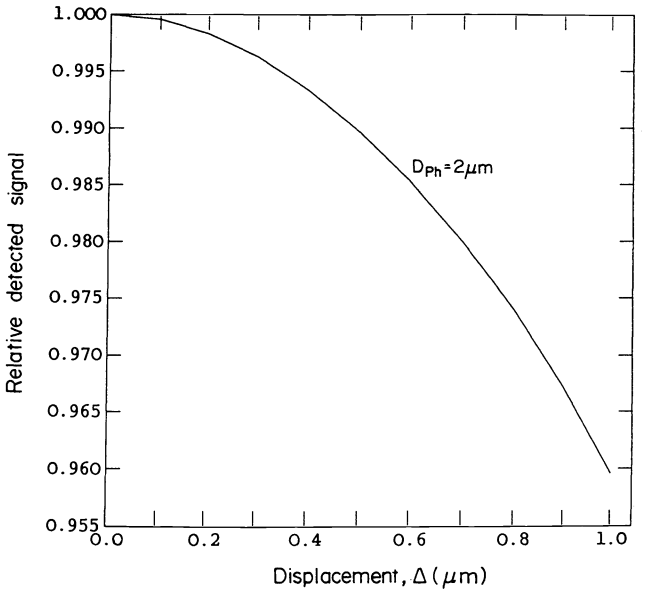

Fig. 6 The detected signal as a function of sample displacement for a pinhole diameter of 2 μm.

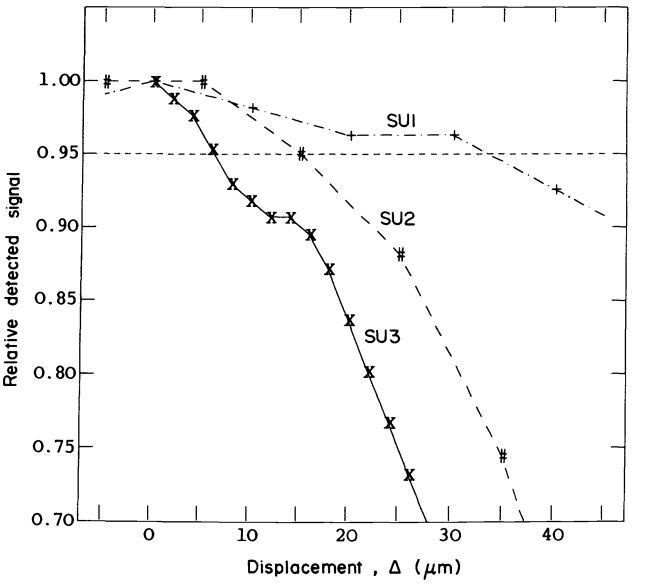

Fig. 8 The measured detected signal as a function of sample displacement for the three different system geometries.

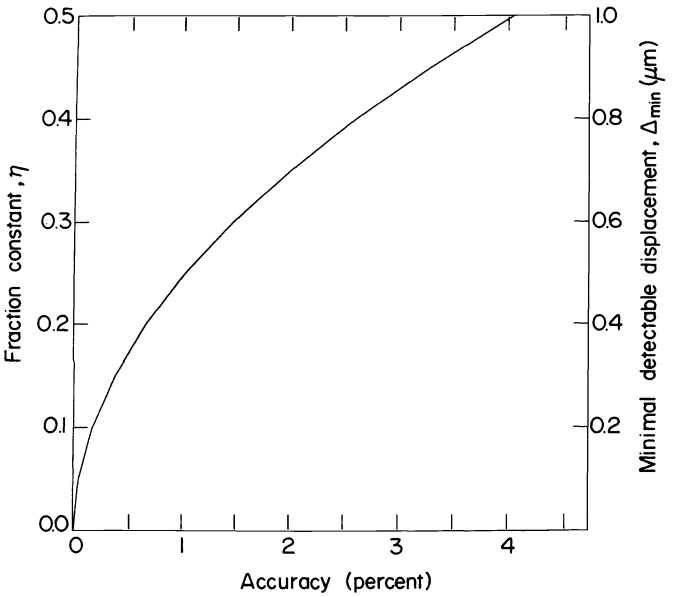

Fig. 7 The fraction constant η and minimal detected displacement as a function of detector accuracy.

was 200 μJ/cm^2, and the resulting diffraction efficiency was approximately 40%.

Three different geometries were used for recording three independent MHOEs. The parameters for the first geometry, denoted by SU1, were chosen to be $D = 2.3$ cm, $R_S = 12$ cm, $R_D = 14$ cm, $D_{ph} \simeq 25$ μm, and the distance from the laser source L to the MHOE, denoted as R_L, was $R_L = 14$ cm. Thus, $f_{\#S} = 5.2$ and $f_{\#D} = 6$. For the second geometry, denoted by SU2, the parameters were chosen to match those of SU1, except for $D_{ph} \simeq 12.5$ μm. The parameters for the third geometry, denoted by SU3, were chosen to be $D = 2$ cm, $R_S = 4$ cm, $R_D = 3$ cm, $R_L = 7$ cm, and $D_{ph} \simeq 5$ μm. In this case $f_{\#S} = 2$ and $f_{\#D} = 1.5$. In all three geometries, the angles between the central ray of the spherical wave converging to S, and the central rays of the spherical waves emerging from P and L are $+45°$ and $-45°$ respectively. The spherical waves emerging from P and L were constructed by microscope objectives, whereas the spherical waves converging to S were formed by high-quality focusing lenses.

The three different MHOEs were independently incorporated into the system shown in Fig. 1, so we could evaluate the system as a function of various MHOE parameters. The sample was either a mirror or a nonpolished aluminum plate and it was displaced with the aid of a stepper motor having 1-μm resolution. In each case we measured the detected signal as a function of sample displacement. The results for the three systems, each with a different MHOE, are presented in Fig. 8. As expected, the resolution of measurement is better for the system using the smaller pinhole diameter for the detector. For example, the minimal detectable displacement Δ_{min} for a detector accuracy of 5% (represented by the horizontal dashed line in Fig. 8) is about ±30 μm for SU1, about ±15 μm for SU2, and about ±6 μm for SU3.

Using Eq. (6) and the experimental results for Δ_{min}, we calculated the fraction constant η for the three systems. For the SU1 and SU2 systems, each having the same parameters except for the different pinhole diameters, the calculated η was the same, about 0.5, for both. This indicated that Δ_{min} is proportional to the diameter of the pinhole, as expected. For the SU3 system, η was about 0.9. The reason for the increase of η, in this case, is probably due to the higher effects of system instabilities when working with lower f numbers and smaller pinholes.

5 Possible System Modifications

For a practical system, use of a laser diode operating in near infrared radiation, instead of a gas laser, is preferred. Unfortunately, available holographic recording materials are not sensitive to infrared radiation, so it is necessary to over-

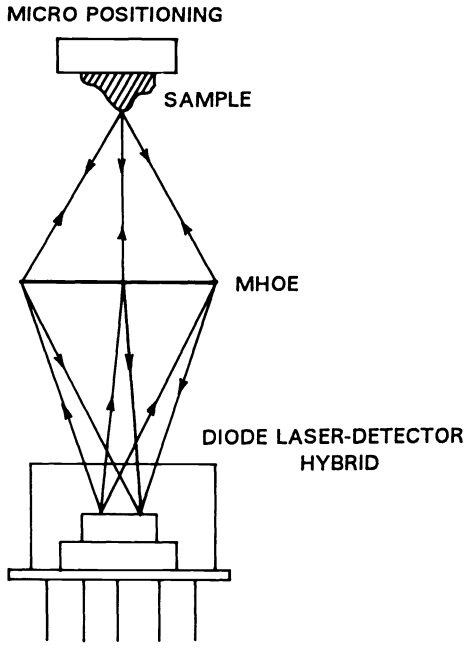

Fig. 9 A possible compact optical system based on a diode laser-detector hybrid device.

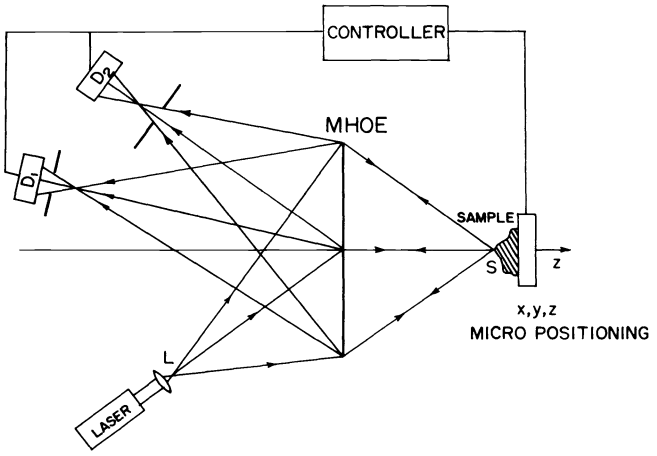

Fig. 10 Modified system configuration.

come the aberrations caused by the wavelength shift between the recording and the readout. For our case of a single image point hologram, this can be done by using a readout geometry that is different from the recording geometry or by using a computer-generated hologram.[10,11] A possible compact optical system is presented in Fig. 9, using a diode laser-detector hybrid device. Here, the diode laser and the detector may be fabricated on the same substrate, using VLSI technology.[5]

Two additional modifications improve the performance of the surface profile measurements system. The first is described with the aid of Fig. 10. The MHOE contains three independent spherical focusing elements instead of only two in the basic system. The first element focuses the light from the laser onto the sample, while the other two elements focus the light reflected from the sample into two detector assemblies (D_1, D_2) with small apertures. One of the detectors is placed a short distance (typically several microns) behind the recording focal plane, while the second detector is placed the same distance in front of it. By comparing the signals from the two detectors, the magnitude can be measured as well as the sign of the defocus. Moreover, differential detection can improve the electronic feedback system and decrease the sensitivity to intensity changes of the laser.[6]

A second modification for the system is based on an astigmatic error detection technique. Here an astigmatic beam (instead of perfect spherical wave) is focused on a quadrodetector (instead of a pinhole and a single detector).[5] The MHOE is almost identical to the basic one, where the astigmatic beam can be generated by using a readout geometry different from the recording geometry or by using computer-generated holograms.

6 Conclusions

We presented a simple and compact noncontact electro-optical system that can measure surface profiles with a high resolution. The simplicity of the system can be attributed to the single low f number MHOE, which combines several different functions in a single hologram that has low aberrations. The system can be further improved by using two detector assemblies with small apertures or using astigmatic error detection techniques.

References

1. R. Thulmann and R. Dändliker, "Holographic contouring using electronic phase measurements," *Opt. Eng.* **24,** 930–935 (1985).
2. F. P. Chiang and D. W. Li, "Random (speckles) patterns for displacement and strain measurement: some recent advances," *Opt. Eng.* **24,** 936–943 (1985).
3. O. Kafri and I. Glatt, "Moire deflectometry: a ray deflection approach to optical testing," *Opt. Eng.* **24,** 944–960 (1985).
4. G. Bickel, G. Häusler, and M. Maul, "Triangulation with expanded range of depth," *Opt. Eng.* **24,** 975–977 (1985).
5. W. H. Lee, "Holographic optical head for compact disk applications," *Opt. Eng.* **28,** 650–653 (1989).
6. Y. Fainman, E. Lenz, and J. Shamir, "Optical profilometer: a new method for high sensitivity and wide dynamic range," *Appl. Opt.* **21,** 3200–3208 (1982).
7. T. R. Corle, C. H. Chou, and G. S. Kino, "Depth response of confocal optical microscopes," *Opt. Lett.* **11,** 770–772 (1986).
8. M. Born and E. Wolf, *Principles of Optics,* Pergamon Press, New York (1965).
9. J. W. Goodman, *Introduction to Fourier Optics,* McGraw-Hill, New York (1968).
10. Y. Amitai, A. A. Friesem, and V. Weiss, "Designing holographic lenses with different recording and readout wavelengths," *J. Opt. Soc. Am. A* **7,** 80–86 (1990).
11. K. Winick, "Designing efficient aberration-free holographic lenses in the presence of a construction-reconstruction wavelength shift," *J. Opt. Soc. Am.* **72,** 143–148 (1982).

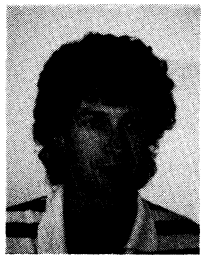

Erez Hasman received the B.Sc. degree in 1981 from the Tel Aviv University, and the M.Sc. degree in 1985 from the Technion, Haifa. From 1981 to 1986, he was employed by the government of Israel, Department of Science, Haifa. Presently, he is at the end of his doctorate at the Weizmann Institute of Science, Rehovot, Israel. His research interests include holography, holographic optical elements, binary optics, far infrared applications, optical computing, optical measurements, and spatial light modulators.

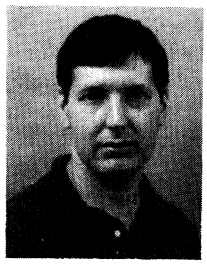

Nir Davidson received the B.Sc. degree in 1982 from the Hebrew University, Jerusalem, and the M.Sc. degree in 1987 from the Technion, Haifa. From 1982 to 1985 he was employed by the government of Israel, Department of Science, Haifa. Presently, he is pursuing his doctorate at the Weizmann Institute of Science, Rehovot. His research interests include holography, holographic optical elements, optical computing, optical measurements, and SLMs.

A. A. Friesem received the B.Sc. and Ph.D. degrees from the University of Michigan in 1958 and 1968, respectively. From 1958 to 1963 he was employed by Bell Aero Systems Company and Bendix Research Laboratories. From 1963 to 1969 he was at the University of Michigan Institute of Science and Technology, conducting investigations in coherent optics, mainly in the areas of optical data processing and holography. From 1969 to 1973 he was principal research engineer in the Electro-Optics Center of Harris, Inc., performing research in the areas of optical memories and displays. In 1973 he joined the staff of the Weizmann Institute of Science, becoming professor of optical sciences in 1977. He is concerned with new holographic concepts and applications, optical image processing, and optical fibers. Friesem is a fellow of OSA, a senior member of IEEE, past chairman of the Israel Laser and Electro-Optics Society, and a member of Eta Kappa Nu and Sigma Xi.